



Understanding summertime H₂O₂ chemistry in North China Plain through observations and modelling studies

Can Ye¹, Pengfei Liu^{2*}, Chaoyang Xue^{3*}, Chenglong Zhang², Zhuobiao Ma², Chengtang Liu², Junfeng Liu², Keding Lu⁴, Yujing Mu^{2*}, Yuanhang Zhang⁴

¹ School of Environmental Science and Engineering, Tiangong University, Tianjin 300387, China

² Research Center for Eco-Environmental Sciences, Chinese Academy of Sciences, Beijing 100085, China

³ Max Planck Institute for Chemistry, Mainz 55128, Germany

⁴ State Key Joint Laboratory of Environment Simulation and Pollution Control, College of Environmental Sciences and Engineering, Peking University, Beijing, 100871, China

Correspondence to: Pengfei Liu (pfliu@rcees.ac.cn), Chaoyang Xue (ch.xue@mpic.de), Yujing Mu (yjmu@rcees.ac.cn)

Abstract.

Hydrogen peroxide (H₂O₂) is a key atmospheric oxidant, crucial for oxidation capacity and sulfate production. However, its chemistry remains understudied compared to ozone (O₃), limiting our understanding of photochemical pollution. In summer 2016, atmospheric peroxides and trace gases were measured at a rural site in the North China Plain. H₂O₂ was the dominant peroxide (0.62 ppb), constituting 69% of total peroxides. It exhibited diurnal variation similar to peroxyacetyl nitrate (PAN) and O₃, indicating photochemical production. The O₃/H₂O₂ ratio was higher on high-particle days, suggesting H₂O₂ uptake by particles reduces its concentration. A box model with default gas-phase chemistry overestimated H₂O₂ by a factor of 2.7, but including particle uptake (uptake coefficient: 6×10⁻⁴) improved agreement with observations.

HO₂ recombination contributed 91% of H₂O₂ production, with a peak rate of 1 ppb h⁻¹. Major removal pathways included particle uptake (69%), dry deposition (25%), OH reaction (4%), and photolysis (2%). Relative incremental reactivity (RIR) analysis showed that reducing NO_x, PM_{2.5}, and alkanes increased H₂O₂, while reducing alkenes, aromatics, CO, and HONO decreased it, with alkenes having the strongest effect. H₂O₂/NO_z ratios (>0.15 in 82% of cases) indicated O₃ formation was in a transition and NO_x-sensitive regime, emphasizing the need for VOC and further NO_x reductions to mitigate both H₂O₂ and O₃ pollution. These findings improve our understanding of H₂O₂ chemistry and provide insights for mitigating photochemical pollution in rural North China.

1 Introduction

The atmospheric oxidation capacity is a critical determinant of atmospheric self-cleaning, influencing the residence time and persistence of pollutant gases. Quantifying this capacity is essential for elucidating the lifetimes of pollutants, the formation of aerosols, and their subsequent radiative forcing effects. Hydrogen peroxide (H₂O₂) serves as a significant atmospheric oxidant, primarily generated through the recombination of hydroperoxyl radicals (HO₂), which are themselves derived from



reactions involving hydroxyl radicals (OH), volatile organic compounds (VOCs), and carbon monoxide (CO). Consequently, the formation of H_2O_2 is intrinsically linked to atmospheric oxidation capacity, with its concentration serving as a direct indicator of the intensity of this capacity. Furthermore, as H_2O_2 represents a terminal product in the ozone (O_3) formation chain reaction, its concentration can be utilized to assess the sensitivity of O_3 production to precursors (Sillman, 1995; Reeves and Penkett, 2003; Nunnermacker et al., 2008; He et al., 2010). Owing to its strong oxidative potential and high Henry's law constant, H_2O_2 readily dissolves in cloud droplets, where it oxidizes sulfur dioxide (SO_2) to form sulfuric acid (H_2SO_4), thereby contributing to sulfate aerosol formation and acid rain deposition (Calvert et al., 1985). Research indicated that H_2O_2 -mediated oxidation of SO_2 in cloud water accounts for 60-80% of global SO_2 oxidation (Penkett et al., 1979; Calvert et al., 1985; Sofen et al., 2011). Additionally, recent studies have highlighted the significant role of particle-phase H_2O_2 oxidation in sulfate formation during winter (Ye et al., 2018; Ye et al., 2021b; Gao et al., 2024). Given its potent oxidative properties, H_2O_2 also poses substantial risks to human health and vegetation (Chen et al., 2010). Thus, a precise understanding of H_2O_2 chemistry is imperative for advancing knowledge of atmospheric oxidation processes and for diagnosing underlying secondary pollution formation mechanisms.

Atmospheric H_2O_2 concentrations are currently reported to range from 0.1 to 13 ppb (Balasubramanian and Husain, 1997; Walker et al., 2006; Ren et al., 2009; Guo et al., 2014; He et al., 2010; Qin et al., 2018; Fischer et al., 2015; Fischer et al., 2019; Ye et al., 2022; Allen et al., 2022; Zhang et al., 2018), with their spatial and temporal variability governed by a balance between production sources and removal pathways. H_2O_2 is generated through both primary and secondary sources. Primary sources of H_2O_2 include biomass burning, which can contribute substantially under specific conditions. For instance, Ye et al. (2022) reported elevated H_2O_2 concentrations during biomass combustion events, which promote secondary sulfate formation and thereby increase fine particulate matter ($\text{PM}_{2.5}$) concentrations. The dominant secondary source is the recombination of HO_2 radicals, a process enhanced during summer months due to increased solar radiation, which elevates HO_2 concentrations and consequently leads to higher H_2O_2 levels. However, under elevated nitrogen oxide (NO_x) conditions, nitric oxide (NO) reacts competitively with HO_2 , suppressing H_2O_2 formation and resulting in reduced atmospheric concentrations. Another secondary source involves the ozonolysis of alkenes, which produces Criegee intermediates that can decompose to form H_2O_2 (Becker et al., 1990). This pathway is particularly relevant during nighttime and potentially in winter, when photochemical activity is diminished (Lee et al., 2008b). For example, alkene ozonolysis was found to dominate wintertime H_2O_2 levels (>70%) (Qin et al., 2018), although the yields are generally low, often below 10%. Additionally, the release of H_2O_2 from the particle phase has been proposed as a potential source, though its contribution is considered negligible compared to gas-phase production. Recent studies, however, have highlighted that under polluted conditions, high concentrations of humic-like substances and transition metals can facilitate particle-phase H_2O_2 formation, which subsequently partitions into the gas phase, significantly enhancing gas-phase H_2O_2 levels (Ye et al., 2021b; Liu et al., 2021).



H_2O_2 can be removed by photolysis, which not only depletes H_2O_2 but also serves as a source of hydroperoxyl radicals (HOx). However, due to lower photolysis frequency, the contribution of H_2O_2 photolysis to atmospheric HOx production is generally much smaller compared to photolysis of O_3 , nitrous acid (HONO), and formaldehyde (HCHO). Notably, particle-phase H_2O_2 photolysis has been identified as a critical source of free radicals within aerosols, accelerating aerosol aging and promoting the formation of secondary pollutants. Rao et al. (2023) further emphasized a significantly accelerated rate for air-water interface H_2O_2 photolysis, underscoring its importance as a source of particle-phase OH . Dry deposition is another key removal mechanism, leading to a vertical gradient in H_2O_2 concentrations, with peak levels observed at approximately 2 km above the surface (Watanabe et al., 2016; Klippel et al., 2011). Due to its high solubility, wet deposition through rainwater scavenging also effectively removes H_2O_2 from the atmosphere. Moreover, laboratory and field studies have demonstrated that heterogeneous uptake by particles can significantly contribute to H_2O_2 removal under polluted conditions. Qin et al. (2022) reported a maximum uptake coefficient of 2.49×10^{-3} for H_2O_2 by ambient particles, with the uptake coefficient influenced by the concentration of transition metals within the particles.

In addition to H_2O_2 , the atmosphere contains a variety of organic peroxides, such as methyl hydroperoxide (CH_3OOH), formed through reactions between HO_2 and organic peroxy (RO_2) radicals. While H_2O_2 is the most abundant peroxide in the atmosphere, organic peroxides are recognized as a significant component of secondary organic aerosol (SOA), contributing to aerosol composition and properties. However, due to analytical challenges associated with measuring organic peroxides, most studies on atmospheric peroxides have only focused on H_2O_2 (Zhang et al., 2012).

Photochemical pollution has emerged as a critical air quality issue in China, impacting both urban and rural regions. H_2O_2 and O_3 are key products of photochemical pollution, and elucidating their chemical behavior is essential for developing effective strategies to mitigate photochemical pollution. However, compared to the extensive research on O_3 , studies on H_2O_2 remain limited due to the technical challenges and complexities associated with its measurement. In recent years, O_3 concentrations in the North China Plain have exhibited a significant upward trend (Li et al., 2019; Wang et al., 2020; Lu et al., 2020), yet the characteristics of H_2O_2 in this region remain poorly understood. Furthermore, the implementation of national emission reduction policies has led to a substantial decline in NOx , while VOCs persist at elevated levels (Liu et al., 2023). This shift toward low NOx and high VOCs conditions is more conducive to H_2O_2 formation. Although photochemical pollution is traditionally considered as an urban phenomenon, recent studies have highlighted its increasing prevalence in rural areas, where pollution levels are gradually approaching those observed in urban areas (Ma et al., 2016). Rural regions typically exhibit lower NOx concentrations than urban areas, creating conditions more favorable for H_2O_2 production. Despite this, research on H_2O_2 in rural areas of the heavily polluted North China Plain remains scarce. Consequently, there is an urgent need to investigate H_2O_2 chemistry in rural environments to inform targeted control strategies for photochemical pollution.



100 This study is based on a field campaign conducted in a rural area of the North China Plain, during which a comprehensive suite of gaseous (including H_2O_2), particulate matter, and meteorological parameters, were measured. Here we investigate the temporal variations of H_2O_2 , and its relationships with other oxidants (e.g., O_3 and peroxyacetyl nitrate, PAN), and preliminarily estimate organic peroxide concentrations. A zero-dimensional box model was employed to examine the influence of particles on the H_2O_2 budget and the sensitivity of H_2O_2 production to various chemical species. Finally, we
105 explore the potential of H_2O_2 as an indicator for determining O_3 sensitivity and discuss the control strategy for alleviating photochemical pollution.

2 Experiments

2.1 Measurement site

The observational experiment was conducted at the Station of Rural Environment, Research Center for Eco-Environmental
110 Sciences (SRE-RCEES, $38^\circ42'\text{N}$, $115^\circ15'\text{E}$), located in Dongbaituo Village, Wangdu County, Hebei Province. Situated approximately 180 km southwest of Beijing, the station is surrounded primarily by farmland with no nearby industrial facilities, making it an ideal site for studying typical rural atmospheric conditions. This location has historically served as a key site for numerous large-scale observational campaigns (Tan et al., 2017; Peng et al., 2021). The experiment took place from 6 July 2016 to 12 August 2016, with the primary objective of investigating the underlying causes of photochemical
115 pollution in the rural North China Plain.

2.2 H_2O_2 measurements

H_2O_2 concentrations were measured using the AL-2021 H_2O_2 monitor (Aero-Laser) (Lazrus et al., 1986). The instrument operates on the following principle: gas-phase peroxides in ambient air are collected by buffered solution in a glass stripping coil. The trapped peroxides then react with p-hydroxyphenyl acetic acid (POPHA) under the catalysis of peroxidase,
120 producing a fluorescent dimer. This dimer exhibits maximal light absorption at a characteristic wavelength of 320 nm and emits fluorescence with a central wavelength of 400 nm. By continuously monitoring the intensity of this fluorescence signal, the instrument enables online quantitative detection of atmospheric peroxides. To differentiate between H_2O_2 and organic peroxides, a dual-channel measurement approach was employed. Channel A measures the total peroxide content, while Channel B incorporates catalase into the absorbent solution to selectively decompose H_2O_2 , thereby measuring only organic
125 peroxides. The H_2O_2 concentration is determined by the difference in signals between the two channels. Although Channel A provides an approximation of total atmospheric peroxides, it should be noted that not all organic peroxides are as efficiently absorbed as H_2O_2 , resulting in an underestimation of total organic peroxide concentrations. The detection limit of the H_2O_2 measurement instrument is 50 ppt, with an uncertainty of 10%. To ensure the stability of the instrument's operation, regular calibrations are performed at fixed intervals. In several previous field experiments (Ye et al., 2018; Ye et al., 2021b; Ye et al.,



2021a; Liu et al., 2021), this instrument has been successfully utilized to measure atmospheric H₂O₂, demonstrating high reliability and consistent operational stability.

2.3 Other species

NO_x, O₃, SO₂, PM_{2.5}, CO, and total reactive nitrogen (NO_y) were measured using commercial instruments from Thermo Electron. Volatile organic compounds (VOCs) were quantified by gas chromatography with a flame ionization detector (GC-FID), while nitrous acid (HONO) was measured using a long-path absorption photometer (LOPAP) from QUMA. The aerosol surface area density was calculated by combining data from a scanning mobility particle sizer (SMPS) and an aerodynamic particle sizer (APS). PAN was analyzed using gas chromatography with electron capture detection (GC-ECD). Gas-phase meteorological data were collected using a portable meteorological station (Model WXT520, Vaisala, Finland). The photolysis rate constant of NO₂ ($j(\text{NO}_2)$) was measured directly, and other photolysis rate constants were derived using the Tropospheric Ultraviolet and Visible (TUV) radiation model, scaled based on $j(\text{NO}_2)$ measurements. Detailed information on the experimental instruments is provided in Table S1.

2.4 Box model descriptions

A zero-dimensional box model based on the RACM2-LIM1 mechanism was employed to investigate the sources and removal mechanisms of H₂O₂. This model is widely recognized for its ability to accurately model HO_x radicals (Tan et al., 2017; Ma et al., 2022). Given that the HO₂ is a critical precursor for H₂O₂ formation, the model's strong performance in simulating free radicals provides confidence in its ability to reliably simulate H₂O₂ concentrations. The model was constrained using input parameters including photolysis rate constants ($j(\text{NO}_2)$, $j(\text{O}^1\text{D})$, $j(\text{HONO})$, $j(\text{H}_2\text{O}_2)$, $j(\text{HCHO})$), VOCs, NO, NO₂, O₃, HONO, methane (CH₄), CO, and meteorological data (temperature, relative humidity, and pressure). VOCs were categorized into different reactivity-based groups according to their reaction rates with OH, as detailed in Table S2. The dry deposition rate constant for H₂O₂ was set to $3 \times 10^{-5} \text{ s}^{-1}$, and boundary layer heights were derived from the hybrid single-particle lagrangian integrated trajectory (HYSPLIT) model.

The simulation focused on the period from 24 July to 3 August, selected for its stable meteorological conditions, characterized by low wind speeds and predominantly static weather. During this period, the observed trends in H₂O₂ concentrations exhibited consistent patterns, suggesting that local photochemical processes were the primary source of H₂O₂. This makes the selected timeframe ideal for exploring H₂O₂ sources using the box model. Additionally, elevated PM_{2.5} concentrations during this period provided an opportunity to investigate the potential influence of particle uptake on H₂O₂ removal. The rate coefficient of H₂O₂ uptake by particles was parameterized as equation 1:

$$k = 0.25 \times c \times \gamma \times S_a \quad \text{Eq. 1}$$

Here c is mean molecular speed of H₂O₂, γ is the H₂O₂ uptake coefficient, and S_a is aerosol surface area density.



To assess the contributions of different precursors to H₂O₂ production, Relative Incremental Reactivity (RIR) analysis was
160 conducted. RIR was calculated using the following equation:

$$\text{RIR}(X) = \frac{\frac{\Delta H_2O_2(X)}{H_2O_2}}{\frac{\Delta C(X)}{C(X)}} \quad \text{Eq. 2}$$

In Eq.2, X represents the primary pollutants that may influence H₂O₂ concentrations. H₂O₂ represents modelled H₂O₂ in the
base case. $\Delta C(X)/C(X)$ represents the relative change of primary pollutants. $\Delta H_2O_2(X)/H_2O_2$ represents the relative change
of modelled H₂O₂ concentrations induced by the reduction of X. Considering the variations in simulated radical
concentrations and the deviations in the RIR, a 20% reduction scenario was selected for further analysis. This approach
165 allowed for the quantification of the sensitivity of H₂O₂ production to variations in precursor concentrations, providing
insights into the key drivers of H₂O₂ formation in the rural North China Plain.



3 Results and discussion

3.1 Time series overview

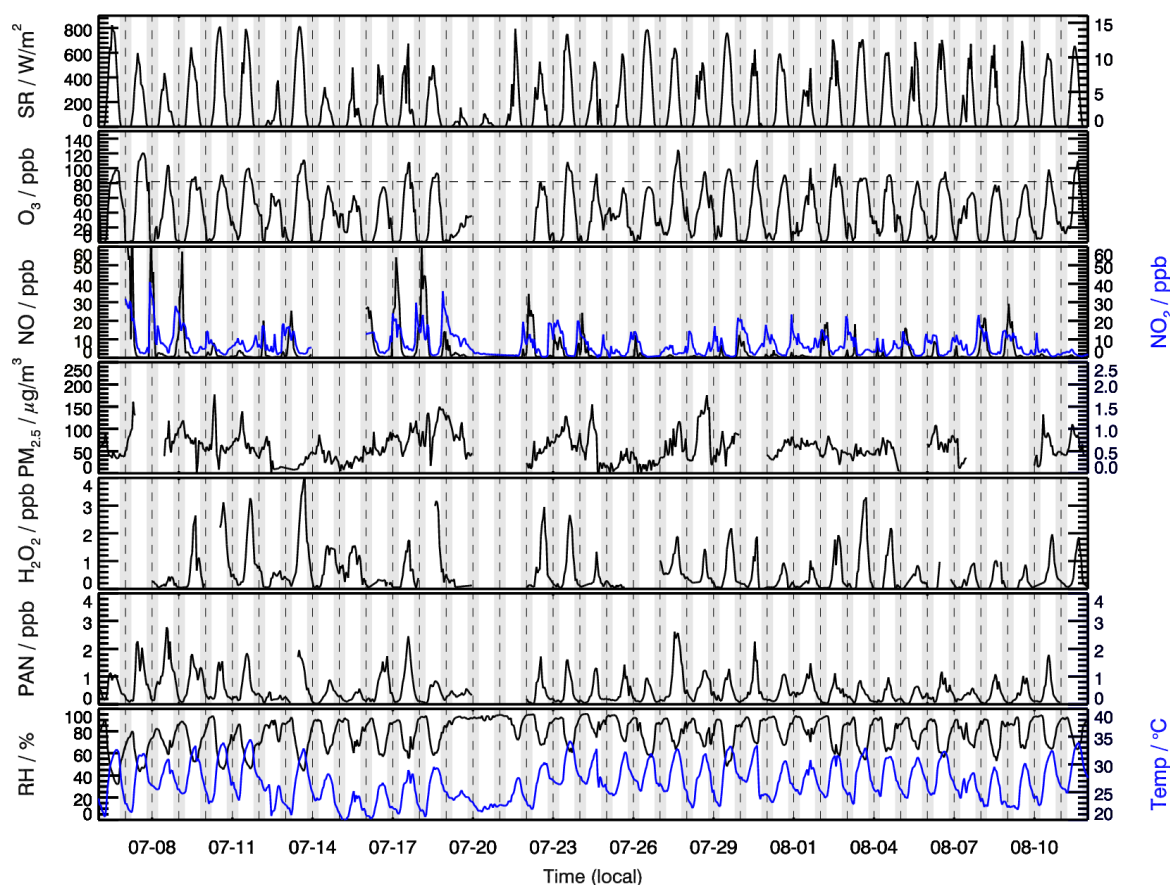


Figure 1. Measurements of H_2O_2 , other related chemical species and meteorological parameters at SRE-RCEES site during the observation period.

Throughout the observation period, meteorological conditions were characterized by high temperature and relative humidity. High temperature generally increased the rate constants of photochemical reactions, while abundant water vapor enhanced the recombination rate of HO_2 and the reaction rate between O^1D and water vapor (H_2O). The maximum O_3 concentration reached 120 ppb, with the maximum daily 8-hour average (MDA8) frequently exceeding the National Ambient Air Quality Standard (NAAQS) Class-II standard of 82 ppb (25 °C, 1013 kPa). High O_3 pollution events often coincided with elevated H_2O_2 concentrations (>2 ppb), suggesting that O_3 production at this site may be sensitive to NO_x . This hypothesis will be further investigated using the $\text{H}_2\text{O}_2/\text{NO}_x$ and O_3/NO_x in Section 3.6 on O_3 sensitivity. NO_x concentrations peaked in the morning, driven by factors such as traffic emissions and lower boundary layer height. Daytime NO concentrations were generally below 1 ppb, while daily peak H_2O_2 concentrations exhibited significant day-to-day variability, ranging from



approximately 0.2 ppb to 4 ppb. Higher H₂O₂ concentrations were observed during periods of intense solar radiation, indicating that local photochemical reactions play a significant role in H₂O₂ production. Notably, elevated H₂O₂ levels were only observed when NO concentrations were low, consistent with the known mechanism of H₂O₂ formation under low NO_x conditions.

185

The average H₂O₂ concentration during the whole observation period was 0.62±0.80 ppb, significantly higher than wintertime concentrations (0.19 ppb) at the same site (Ye et al., 2021b), as summer conditions with high solar radiation intensity and relative humidity are more conducive to H₂O₂ production. This average concentration also exceeded summer H₂O₂ levels reported in urban areas, such as Beijing (0.27 pb) (Qin et al., 2018) and Hongkong (0.32 ppb) (Guo et al., 2014), likely due to lower NO_x levels at the rural site, which favor H₂O₂ formation. Compared to H₂O₂ concentrations reported at rural sites in other countries, the levels observed in this study were lower than that in Kinterbish (Watkins et al., 1995), Whiteface Mountain (1.61 ppb) (Balasubramanian and Husain, 1997). It is worth mentioning that, an average H₂O₂ concentration of 0.51±0.90 ppb was reported at the same site in summer 2014 (Wang et al., 2016), lower than the current study's findings, reflecting a potential increasing trend in H₂O₂ concentrations over time. In addition, multi-year measurements at the summit of Mount Tai revealed an increasing trend of H₂O₂ concentrations in cloud water from 2014 to 2018 (Li et al., 2020), indirectly indicating rising gas-phase H₂O₂ levels in the North China Plain.

Elevated H₂O₂ concentrations and high relative humidity in rural areas facilitate the oxidation of SO₂ by H₂O₂ in both aerosol water and cloud water, contributing to sulfate formation and increased PM_{2.5} levels. During the observation period, the average PM_{2.5} concentration reached 57 µg m⁻³, and the co-occurrence of PM_{2.5} and O₃ pollution was frequently observed. This dual pollution phenomenon suggests that high concentrations of oxidants may play a significant role in driving secondary aerosol formation. PAN, another key secondary oxidant measured in this study, reached a maximum concentration of 2.9 ppb. Similar to H₂O₂ and O₃, PAN is a product of photochemical pollution, and its temporal trends closely mirrored those of H₂O₂ and O₃. These trends will be analyzed in detail in the section 3.2. As strong oxidizing agents, H₂O₂, O₃ and PAN are proven to be damaging to vegetation and human health. Given the high concentrations of these oxidants observed in this study, photochemical pollution in rural areas poses serious risks to agricultural productivity and human health.

3.2 Diurnal patterns of three photochemical oxidants

The average diurnal trends of H₂O₂, PAN, and O₃ exhibited pronounced daily variations, with concentrations peaking during the daytime and declining at night (Figure 2). These trends closely followed solar radiation patterns, highlighting the significant contribution of photochemical reactions to their formation. In addition, the pronounced daily variations also indicated the presence of abundant precursors in the region facilitating the production of H₂O₂, PAN, and O₃. In the early morning, as solar radiation intensified, the photolysis of HONO initiated daytime photochemical reactions (R0), generating peroxy radicals (R1). These radicals reacted with NO to produce O₃ (R2-R5); HO₂ recombination underwent bimolecular



recombination to produce H_2O_2 (R6); peroxyacetyl radicals (PA) reacted with NO_2 to form PAN (R7). These processes led to a rapid increase in the concentrations of all three oxidants, with peak concentrations reaching 1.8 ppb, 1.2 ppb, and 84 ppb for H_2O_2 , PAN, and O_3 , respectively.

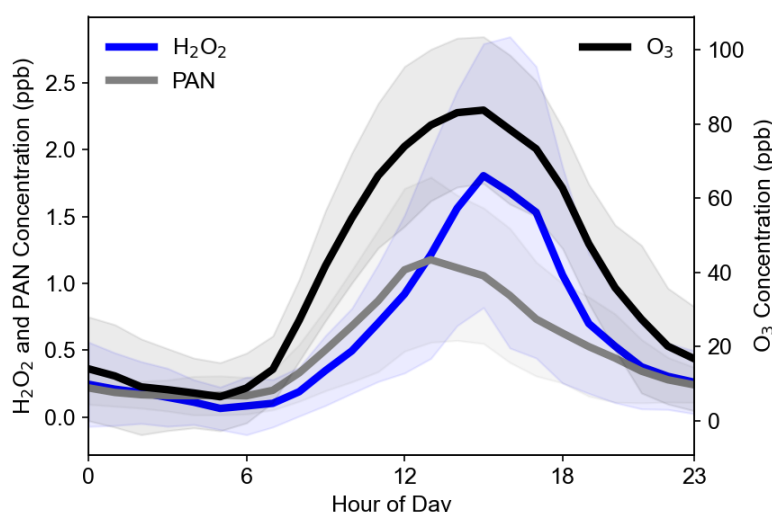
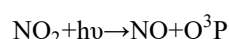
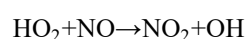
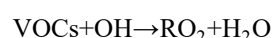
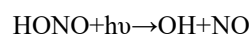
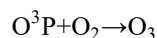


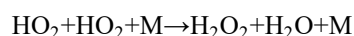
Figure 2. Diurnal cycles of H_2O_2 , PAN and O_3 .

Despite sharing similar photochemical formation pathways, the peak times of the three oxidants differed due to variations in their production and removal rates. PAN concentrations peaked around noon, approximately 2–3 hours earlier than H_2O_2 and O_3 , a phenomenon also observed in previous studies (Lee et al., 2008a). This earlier peak for PAN can be attributed to its higher thermal decomposition rate at midday. In contrast, the peaks for H_2O_2 and O_3 both occurred around 16:00. Notably, in urban areas, H_2O_2 peaks often lag behind O_3 peaks. For example, observations at the urban Tai'an site in the North China Plain revealed that H_2O_2 peaks occurred approximately 2 hours after O_3 peaks (Ye et al., 2021a). This delay can be explained by HO_2 chemistry under varying NO_x conditions. Under high NO_x condition, HO_2 primarily reacts with NO (reaction rate constant: $8.9 \times 10^{-12} \text{ cm}^3 \text{ molecule}^{-1} \text{ s}^{-1}$ at 298 K), whereas under low NO_x condition, HO_2 undergoes bimolecular recombination to form H_2O_2 (reaction rate constant: $1.5 \times 10^{-12} \text{ cm}^3 \text{ molecule}^{-1} \text{ s}^{-1}$ at 298 K). In urban settings, H_2O_2 peaks only occur when NO concentrations drop to around 100 ppt, allowing HO_2 recombination to dominate, thus delaying the H_2O_2 peak relative to O_3 . However, at this rural site, daytime NO concentrations were consistently low, resulting in simultaneous peaks for O_3 and H_2O_2 .

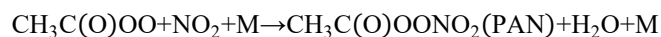




R5



R6



R7

235 Following their peaks, the concentrations of all three oxidants declined rapidly. For H_2O_2 , this decrease was primarily driven by dry deposition and, in the evening, enhanced uptake by liquid aerosols formed as relative humidity increased. O_3 concentrations dropped due to a combination of dry deposition and NO titration, while PAN levels decreased mainly through thermal decomposition. At night, the absence of photochemical reactions caused all three oxidants to maintain low concentrations.

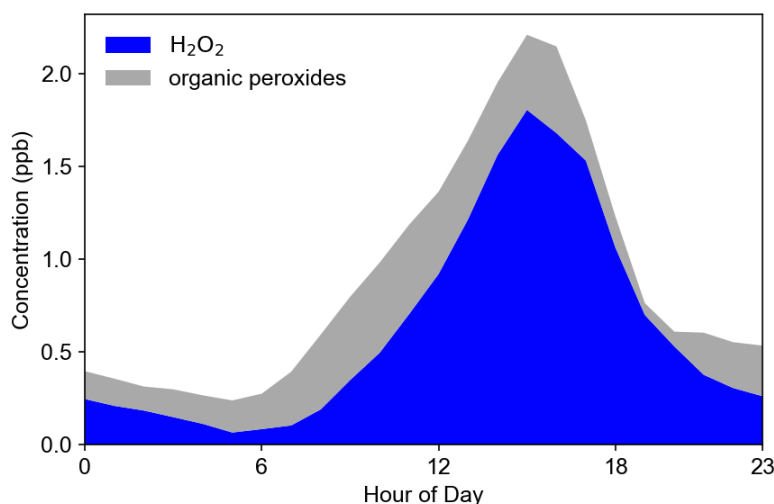


Figure 3. The concentrations of H_2O_2 and organic peroxides.

240

Figure 3 illustrates the average diurnal trends of organic peroxides and H_2O_2 . The trends of total peroxides closely align with those of H_2O_2 , indicating similar production and removal mechanisms. H_2O_2 accounts for 69% of the total peroxides, while organic peroxides (0.28 ppb) constitute 31%. This demonstrates that peroxides in rural areas are predominantly dominated by H_2O_2 , consistent with the findings of Wang et al. (2016) at this site. However, it is important to note that the percentage of organic peroxides reported in this study represents a lower limit, as not all organic peroxides are fully captured by the measurement technique. In contrast, Liang et al. (2013) reported that organic peroxides accounted for 80% of total peroxides in urban areas such as Beijing. The difference in organic peroxide proportions between Beijing and Wangdu can likely be attributed to variations in chemical conditions, such as differences in VOC compositions, which influence the types and abundances of peroxy radicals formed.

250



3.3 Correlations between different atmospheric oxidants

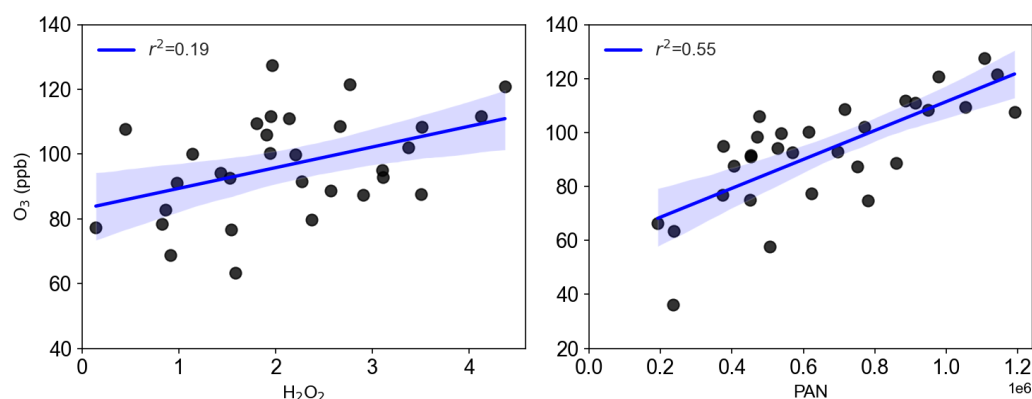


Figure 4. Correlations of O₃ daily maximum with H₂O₂ and PAN daily maximum

255 The formation of H₂O₂, O₃, and PAN is closely linked to VOCs, NO_x, and solar radiation. Consequently, their concentrations are typically elevated and well-correlated during photochemical pollution episodes. Here, we investigate the relationships among these oxidants. Figure 4 illustrates the correlations between the daily maximum concentrations of H₂O₂, O₃, and PAN. A good correlation ($r^2 = 0.55$) was observed between PAN and O₃, consistent with previous studies (Lee et al., 2008a; Zhang et al., 2014; Xu et al., 2021; Sun et al., 2020). In contrast, the correlation between H₂O₂ and O₃ was weak ($r^2 =$
260 0.19). Prior research has shown positive correlations between H₂O₂ and O₃ during photochemical pollution due to their shared dependence on VOC and NO_x photochemistry (Hua et al., 2008; Takami et al., 2003; Ye et al., 2021a; Guo et al., 2022), while negative correlations have been reported in clean marine boundary layer where O₃ photolysis dominates radical production (Ayers et al., 1992). The lack of a positive correlation between O₃ and H₂O₂ in this rural polluted environment may indicate additional factors influencing H₂O₂ concentrations. Notably, heterogeneous uptake by particles has been shown
265 to affect H₂O₂ levels (De Reus et al., 2005; Qin et al., 2018), and given the relatively high PM_{2.5} concentrations during the observation period, we hypothesize that heterogeneous loss reduces gas-phase H₂O₂, weakening its correlation with O₃.

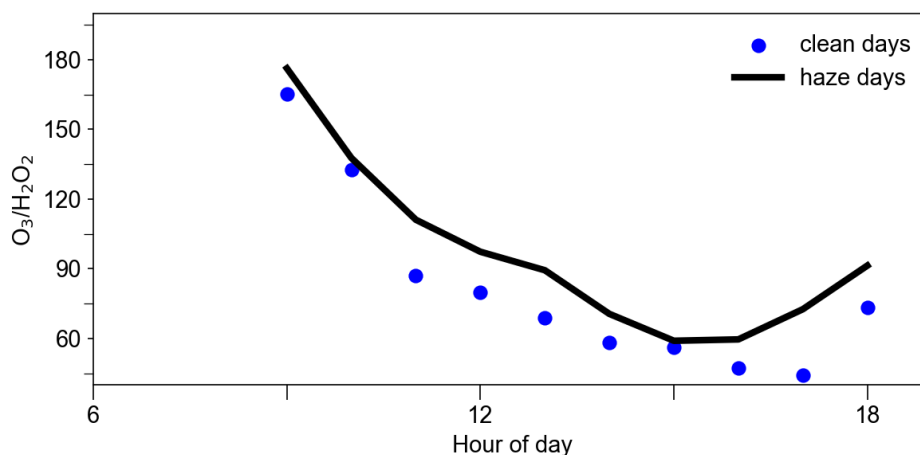


Figure 5. Average O_3/H_2O_2 from 9:00 to 18:00 on clean (daily average $PM_{2.5} < 50 \mu g m^{-3}$) and polluted days (daily average $PM_{2.5} \geq 50 \mu g m^{-3}$).

270 To test this hypothesis, we analyzed the O_3/H_2O_2 ratio on polluted (daily average $PM_{2.5} < 50 \mu g m^{-3}$) and clean days (daily average $PM_{2.5} \geq 50 \mu g m^{-3}$). While O_3 and H_2O_2 share similar photochemical formation pathways, O_3 is less affected by particle uptake. O_3 lifetime was estimated to be 13 days with respect to heterogeneous uptake for dust mass concentrations of $1000 \mu g m^{-3}$, highlighting the minor role of particle uptake on O_3 removal (Tang et al., 2017). If the O_3/H_2O_2 ratio remains stable across polluted and clean conditions, heterogeneous uptake likely has minimal impact on H_2O_2 . However, if the ratio

275 is higher during polluted periods, it is possible that $PM_{2.5}$ may scavenge H_2O_2 by heterogeneous uptake. As shown in Figure 5, the O_3/H_2O_2 ratio during peak photochemical hours (9:00–18:00) was markedly higher on polluted days compared to clean days, supporting the hypothesis that heterogeneous uptake by $PM_{2.5}$ significantly reduces H_2O_2 concentrations. It is important to note that this method provides only a preliminary assessment, as uncertainties exist due to differences in the dependence of H_2O_2 and O_3 on peroxy radical concentrations and their respective responses to radiation intensity. In the

280 following section, we further examine the impact of $PM_{2.5}$ on H_2O_2 budget using a box model.



3.4 Investigation on H₂O₂ budget

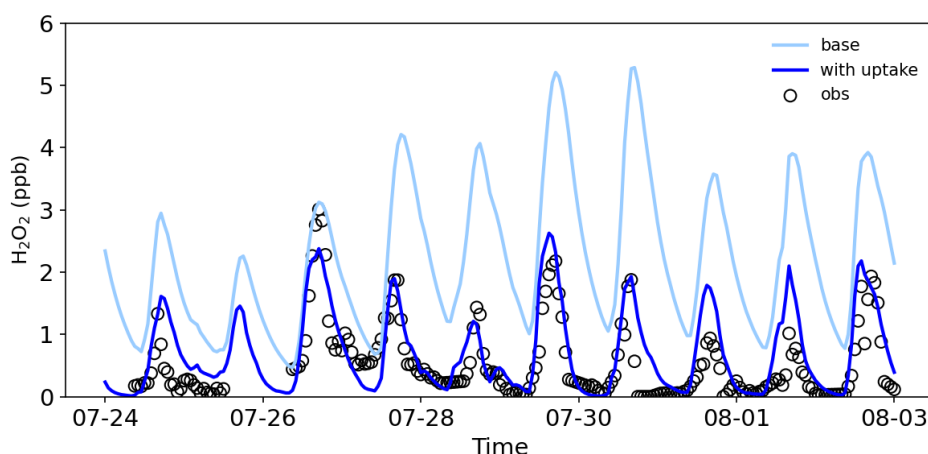


Figure 6. Observed and modelled H₂O₂ concentrations from 24 July to 3 August.

285 To better understand the sources and removal mechanisms of H₂O₂, we employed a box model to simulate its concentrations. As shown in Figure 6, base simulations using the model's default H₂O₂ source and removal mechanisms overestimated H₂O₂ concentrations compared to observations, with a simulated-to-measured ratio of 2.7. This discrepancy suggests an unaccounted removal pathway, consistent with our earlier hypothesis of H₂O₂ removal by particle uptake. When a parameterized uptake mechanism with an uptake coefficient of 6×10^{-4} was incorporated into the box model, the simulated
 290 H₂O₂ concentrations and trends aligned well with observed values (Fig. 6), confirming the significant role of particle uptake in H₂O₂ removal in rural areas. This uptake coefficient is comparable with the value (5×10^{-4}) estimated during a dense Saharan dust event (De Reus et al., 2005), and lower than 1×10^{-3} reported by Wang et al. (2016), which may be likely due to differences in particulate matter composition. Sensitivity tests indicated that an uptake coefficient of 1×10^{-3} resulted in underestimation (Figure.S1), supporting 6×10^{-4} as the optimal value for our study. This coefficient falls within the range (10^{-4} – 10^{-3}) determined in laboratory studies for H₂O₂ uptake on ambient particles collected on filters or artificial particles
 295 (Pradhan et al., 2010; Romanias et al., 2012; Qin et al., 2022).

It should be mentioned that previous studies have demonstrated that considering HO₂ by particles can partially explain the discrepancy between observed and modeled HO₂ concentrations under low NO_x conditions (Kanaya et al., 2007a; Kanaya et al., 2007b; Whalley et al., 2010; Ma et al., 2022), as well as the phenomenon of increasing O₃ concentrations with decreasing
 300 particulate matter levels (Li et al., 2019). Since HO₂ is a precursor to H₂O₂, its uptake by particles naturally reduces H₂O₂ concentrations. However, laboratory-measured HO₂ uptake coefficients exhibit significant variability, ranging from 10^{-5} to 0.82, and are strongly influenced by the composition of particulate matter (Thornton et al., 2008; Taketani et al., 2012; George et al., 2013; Lakey et al., 2015). Through analysis of measured radical budget and related parameters, Tan et al. (2020) showed that the HO₂ uptake was not important in the North China Plain in 2014, with an uptake coefficient of 0.08.



305 Given that our observational experiments were conducted at the same site with similar particulate matter composition, we also assumed an HO₂ uptake coefficient of 0.08 to investigate its impact on the H₂O₂ budget. Under this assumption, we found that an H₂O₂ uptake coefficient of 4.5×10^{-4} resulted in a good agreement between modeled and observed H₂O₂ concentrations (Figure S1). The results indicate that considering HO₂ uptake reduces the H₂O₂ uptake coefficient by 25%. Therefore, uncertainties in the HO₂ uptake coefficient significantly affect the accurate simulation of H₂O₂ concentrations and the estimation of the H₂O₂ uptake coefficient. A more precise parameterization scheme for HO₂ uptake is critical for models to accurately assess the global distribution of H₂O₂ concentrations and their environmental impacts.

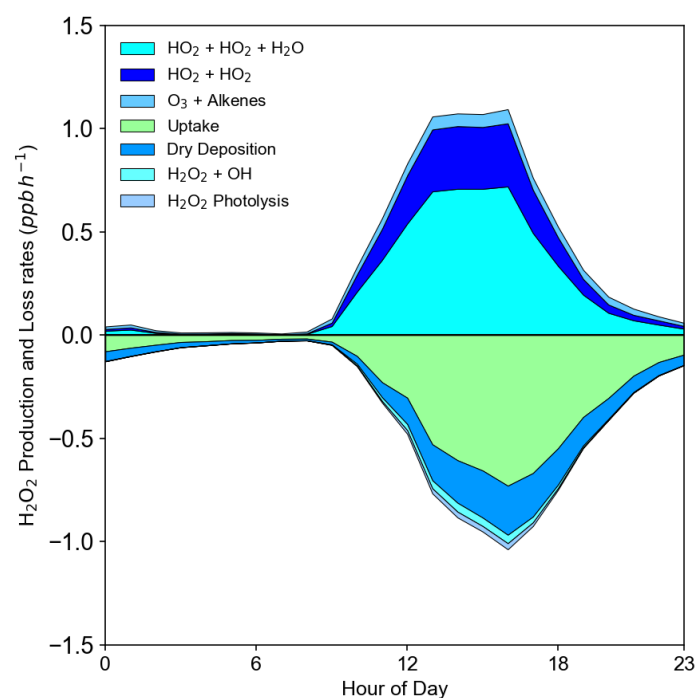


Figure 7. Modelled H₂O₂ sources and sinks.

315 Figure 7 depicts the H₂O₂ production rates and removal rates by different pathways. The percentage contribution of different pathways is shown in Figure S2. HO₂ bimolecular recombination was identified as the dominant H₂O₂ production pathway, contributing to 80% H₂O₂ production with a maximum yield of 1.0 ppb h⁻¹ at noon. This highlighted rapid photochemical production as the primary driver of H₂O₂ pollution in the rural site. In contrast, the reaction of O₃ with alkenes accounted for 9% H₂O₂ production (Figure S2), with a maximum yield of 0.07 ppb h⁻¹, primarily from O₃+OLI reactions. This mechanism was found to be significant during winter pollution due to high alkenes and NO concentrations inhibiting HO₂ recombination (Qin et al., 2018). Heterogeneous uptake dominated H₂O₂ removal, accounting for 64% with a maximum removal rate of 0.7 ppb h⁻¹, underscoring its importance during summer pollution periods. Dry deposition, photolysis, and reaction with OH



radicals contributed to 25%, 1%, and 3% H_2O_2 loss, respectively. These findings provide a comprehensive understanding of H_2O_2 sources and sinks in rural environments, emphasizing the critical role of particle uptake in H_2O_2 budget.

3.5 Precursors control to mitigate H_2O_2 pollution

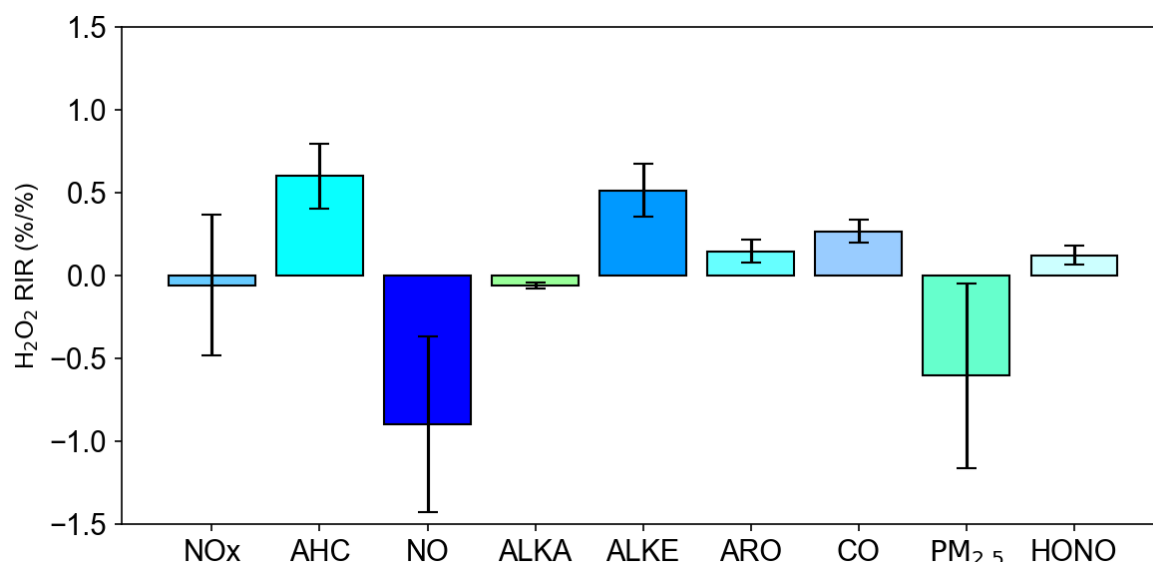


Figure 8. Sensitivity of H_2O_2 production to different chemical species.

It is evident that photochemical pollution in rural areas is associated with elevated concentrations of H_2O_2 , necessitating urgent measures to mitigate H_2O_2 pollution by regulating its precursor compounds. Given the diversity of precursors involved in H_2O_2 formation, a critical objective is to quantify the relative contribution of each precursor to H_2O_2 pollution to establish prioritized control strategies. In this study, the RIR method was employed to identify the most effective pollutants for H_2O_2 control (Figure 8). The results demonstrate that reducing NO concentrations leads to an increase in H_2O_2 levels, as the reaction between NO and HO_2 inhibits H_2O_2 production. However, under realistic conditions, a decrease in NO also results in reduced NO_2 levels. Since the NO_2 heterogeneous reaction is a significant source of HONO, which serves as a key precursor for OH influencing H_2O_2 formation, a decline in NO_2 consequently reduces H_2O_2 concentrations. To validate this hypothesis, RIR values for NOx were calculated. Although the absolute RIR values for NOx remained negative (-0.06), they were significantly lower than those for NO (-0.9), indicating that the reduction in H_2O_2 due to decreased NO_2 partially offsets the increase in H_2O_2 caused by reduced NO.

Furthermore, the negative RIR value for alkanes (-0.06) suggests that lowering alkane concentrations enhances H_2O_2 production, likely due to their lower photochemical reactivities with OH. When alkane levels are reduced, OH radicals preferentially react with more reactive alkenes and aromatics, leading to increased HO_2 and hence more H_2O_2 formation. The



RIR values for alkenes (0.51), aromatics (0.15), and CO (0.26) were consistently positive, indicating that reducing these pollutants is effective in reducing H₂O₂ concentrations, with alkenes exhibiting the most pronounced effect. Consequently, controlling alkenes concentrations within anthropogenic VOCs should be prioritized, aligning with findings from previous studies (Wang et al., 2016; Ye et al., 2021a). Coal combustion and gasoline exhaust were identified as primary sources of alkenes in the region, underscoring the importance of regulating these emissions to mitigate H₂O₂ pollution. Additionally, RIR value for HONO was 0.12, indicating reducing HONO concentrations can further diminish H₂O₂ levels by limiting the primary radical source. Elevated HONO concentrations have been observed across various sites in China, contributing over 40% to primary radical production. Thus, reducing HONO emissions represents a potential mitigating strategy for H₂O₂. Ye et al. (2022) reported that HONO emissions due to fertilizer use significantly increase H₂O₂ levels in rural areas, suggesting that reducing excessive fertilizer use could mitigate H₂O₂ pollution. Moreover, NO₂ heterogeneous reactions at various interfaces and nitrate photolysis are additional sources of HONO (Xue et al., 2020; Xue et al., 2022), highlighting the potential to reduce H₂O₂ by decreasing NO₂ concentrations and subsequently limiting HONO production.

The RIR value for PM_{2.5} (-0.6) was found to be negative, as reducing PM_{2.5} decreases the uptake of H₂O₂, thereby increasing its gas-phase concentration. Recent studies have extensively examined the impact of PM_{2.5} reduction on O₃ concentrations, attributing this phenomenon to diminished HO₂ radical uptake and enhanced photolysis rates, both of which elevate O₃ levels (Wang et al., 2019; Song et al., 2022). These mechanisms similarly contribute to increased H₂O₂ concentrations, yet the effect of particulate matter reduction on H₂O₂ has been largely overlooked. This study demonstrates that PM_{2.5} reduction also decreases H₂O₂ uptake, further exacerbating its gas-phase concentration. This increase in H₂O₂ could enhance sulfate formation efficiency and pose greater threats to human health and ecosystems. Given the critical role of H₂O₂ in atmospheric oxidation capacity, global sulfate aerosol formation, and human health, further research is warranted to investigate H₂O₂ trends, environmental impacts, and mitigation strategies.

3.6 Implications on O₃ formation

H₂O₂ measurements serve as a valuable indicator of O₃ production sensitivity. Under NO_x poor conditions, the HO₂ recombination to form H₂O₂ represents the primary radical termination pathway. Conversely, under NO_x sufficient conditions, the reaction between NO₂ and OH to form nitric acid (HNO₃) constitutes the dominant termination mechanism. Sillman (1995) identified the H₂O₂/HNO₃ ratio as a robust indicator of O₃ sensitivity, with model simulations revealing that a ratio between 0.2 and 0.3 corresponds to a transitional regime, while values exceeding 0.3 indicate NO_x-limited conditions and values below 0.2 suggest VOC-limited conditions. In the absence of direct gaseous HNO₃ measurements, alternative metrics such as H₂O₂/NO_y or H₂O₂/NO_z can be employed to assess O₃ sensitivity (Sillman et al., 1998), where NO_z encompasses HNO₃, PAN, HONO, and alkyl nitrates, and NO_y is defined as NO_z + NO_x.

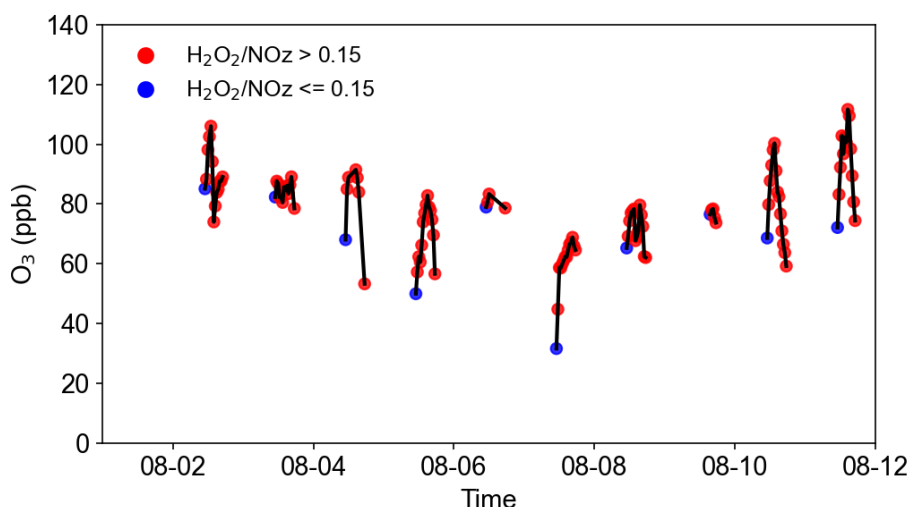


Figure 9. O_3 concentrations values from 1 August to 11 August. The red points represent measurements where H_2O_2/NO_z is greater than 0.15, while the blue points correspond to measurements where H_2O_2/NO_z is less than or equal to 0.15.

In this study, simultaneous measurements of H_2O_2 and NO_z enabled the determination of O_3 sensitivity using the H_2O_2/NO_z ratio, with a transitional range identified at 0.15–0.20 (Sillman et al., 1998). The analysis focused on the period of intense photochemical activity between 10:00 and 17:00. As illustrated in Figure 9, over 82% of measured H_2O_2/NO_z values exceeded 0.15, indicating that the rural study area predominantly exhibited NO_x -limited or transitional conditions during most of the observed period. It is important to note that this metric can be influenced by additional factors. For instance, significant uptake of H_2O_2 by particles was observed in this study, suggesting that the actual photochemical production of H_2O_2 is higher than the measured concentrations. Consequently, the theoretical H_2O_2/NO_z ratio is likely greater than the observed values, implying that O_3 production is more strongly aligned with NO_x -limited or transitional regimes.

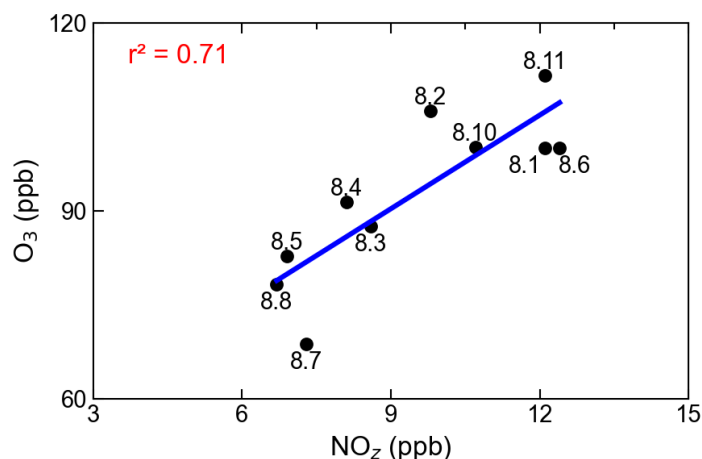


Figure 10. Correlation between daily maxima of O_3 and NO_z . The numbers adjacent to the solid dots represent the dates.



To corroborate these findings, the O_3/NO_z ratio was also utilized to evaluate O_3 sensitivity. The relationship between peak
390 O_3 concentrations and peak NO_z concentrations demonstrated a good positive correlation ($r^2=0.71$), with a regression slope
of 4.98. This slope is comparable with the value (3.3-7.6) reported in a mountainous area north of Beijing (Wang et al.,
2006), but lower than those (6-11) observed in Houston (Daum et al., 2004). Notably, the positive correlation persisted up to
 NO_z concentrations of 12 ppb, differing from observations at other sites where the slope typically decreased for NO_z levels
above 10 ppb (Trainer et al., 1993). This deviation can be attributed to reduced O_3 production efficiency under VOC-limited
395 conditions. However, the sustained positive correlation across the entire study period suggests that the generation of NO_z is
consistently accompanied by O_3 production, further supporting the prevalence of NO_x -sensitive or transitional regimes.
These results align with those derived from the H_2O_2/NO_z ratio, affirming the utility of H_2O_2/NO_z as a reliable indicator of
 O_3 sensitivity.

400 The findings underscore the importance of controlling NO_x concentrations to mitigate photochemical pollution in rural areas.
Tan et al. similarly reported that O_3 production in the rural North China Plain is primarily NO_x -limited. As NO_x emissions
continue to decline due to regulatory efforts, an increasing number of regions may transition into NO_x -limited or transitional
regimes, highlighting the potential benefits of stringent NO_x reduction strategies for future O_3 pollution control. However,
given the need for synergistic management of H_2O_2 and O_3 , a dual approach targeting both NO_x and VOC emissions remains
405 essential. This integrated strategy will be critical for achieving effective and sustainable air quality improvements.

4 Conclusions

To investigate photochemical pollution in rural areas, measurements of H_2O_2 and related parameters were conducted in the
Wangdu region during the summer of 2016. H_2O_2 exhibited a distinct diurnal pattern, with an average concentration of
 0.62 ± 0.80 ppb. Daily maximum concentrations of H_2O_2 varied significantly, ranging from a minimum of 0.2 ppb to a
410 maximum of 4 ppb. The diurnal cycles of H_2O_2 , PAN, and O_3 all followed solar radiation trends, indicating that
photochemical reactions predominantly control their production. A good correlation ($r^2 = 0.55$) was observed between daily
maximum concentrations of PAN and O_3 , whereas the correlation between maximum concentrations of H_2O_2 and O_3 was
weak, suggesting that unidentified processes influencing gas-phase H_2O_2 concentrations may attenuate this relationship.
Analysis of the O_3/H_2O_2 ratio revealed that this ratio was significantly higher on polluted days compared to clean days,
415 implying that particle uptake likely reduces gas-phase H_2O_2 concentrations.

To further elucidate the factors influencing H_2O_2 concentrations, a box model was employed. The model simulations initially
overestimated H_2O_2 concentrations with a modelled-to-observed ratio of 2.7. However, when H_2O_2 heterogeneous uptake
mechanism was incorporated into the model scheme with an uptake coefficient of 6×10^{-4} , the simulated H_2O_2 concentrations
420 aligned well with observed data, underscoring the significant role of heterogeneous uptake in H_2O_2 removal. The primary



source of H_2O_2 was identified as the bimolecular recombination of HO_2 , contributing 91% of the total source strength, with a maximum production rate of 1 ppb h^{-1} . The dominant removal pathways for H_2O_2 included particle uptake (69%), followed by dry deposition (25%), reaction with OH (4%), and photolysis (2%).

425 Relative Incremental Reactivity (RIR) analysis demonstrated that reducing NO_x , $\text{PM}_{2.5}$, and alkanes exacerbated H_2O_2 concentrations, whereas lowering alkenes, aromatics, CO, and HONO effectively reduced H_2O_2 pollution, with alkenes exhibiting the most pronounced impact. The $\text{H}_2\text{O}_2/\text{NO}_x$ ratio and the positive correlation between daily peak O_3 and NO_x concentrations indicated that O_3 production predominantly occurred in transitional and NO_x -limited regimes. To concurrently mitigate H_2O_2 and O_3 pollution, a dual strategy focusing on VOC control and stringent NO_x reduction is
430 essential. This approach will be critical for achieving synergistic control of photochemical pollutants in rural areas.

Data availability. The data used in this study are available from the corresponding author upon request (yjmu@rcees.ac.cn).

Author contributions. YM designed the experiments. CY performed H_2O_2 measurements and analyzed the data. CY wrote the manuscript with input from PL and CX. All authors contributed to measurements, discussing results, and commenting on
435 the manuscript.

Competing interests. The contact author has declared that neither they nor their co-authors have any competing interests.

Acknowledgements. We thank the science teams of the summer campaign for their support.

Financial support. This work was supported by the National Natural Science Foundation of China (grant nos. 42305099, 42275111).
440

References

- Allen, H. M., Bates, K. H., Crounse, J. D., Kim, M. J., Teng, A. P., Ray, E. A., and Wennberg, P. O.: H_2O_2 and CH_3OOH (MHP) in the Remote Atmosphere: 2. Physical and Chemical Controls, *Journal of Geophysical Research: Atmospheres*, 127, e2021JD035702, <https://doi.org/10.1029/2021JD035702>, 2022.
445
Ayers, G., Penkett, S., Gillett, R., Bandy, B., Galbally, I., Meyer, C., Elsworth, C., Bentley, S., and Forgan, B.: Evidence for photochemical control of ozone concentrations in unpolluted marine air, *Nature*, 360, 446-449, 1992.
Balasubramanian, R. and Husain, L.: Observations of gas-phase hydrogen peroxide at an elevated rural site in New York, *J Geophys Res-Atmos*, 102, 21209-21220, Doi 10.1029/97jd01480, 1997.
450
Becker, K. H., Brockmann, K. J., and Bechara, J.: Production of hydrogen peroxide in forest air by reaction of ozone with terpenes, *Nature*, 346, 256-258, 1990.
455
Calvert, J. G., Lazrus, A., Kok, G. L., Heikes, B. G., Walega, J. G., Lind, J., and Cantrell, C. A.: Chemical Mechanisms of Acid Generation in the Troposphere, *Nature*, 317, 27-35, Doi 10.1038/317027a0, 1985.
Chen, X., Aoki, M., Takami, A., Chai, F., and Hatakeyama, S.: Effect of ambient-level gas-phase peroxides on foliar injury, growth, and net photosynthesis in Japanese radish (*Raphanus sativus*), *Environ Pollut*, 158, 1675-1679, 10.1016/j.envpol.2009.12.002, 2010.
460



- Daum, P. H., Kleinman, L. I., Springston, S. R., Nunnermacker, L. J., Lee, Y. N., Weinstein-Lloyd, J., Zheng, J., and Berkowitz, C. M.: Origin and properties of plumes of high ozone observed during the Texas 2000 Air Quality Study (TexAQS 2000), *Journal of Geophysical Research: Atmospheres*, 109, <https://doi.org/10.1029/2003JD004311>, 2004.
- 465 de Reus, M., Fischer, H., Sander, R., Gros, V., Kormann, R., Salisbury, G., Van Dingenen, R., Williams, J., Zöllner, M., and Lelieveld, J.: Observations and model calculations of trace gas scavenging in a dense Saharan dust plume during MINATROC, *Atmos. Chem. Phys.*, 5, 1787-1803, 10.5194/acp-5-1787-2005, 2005.
- 470 Fischer, H., Pozzer, A., Schmitt, T., Jöckel, P., Klippel, T., Taraborrelli, D., and Lelieveld, J.: Hydrogen peroxide in the marine boundary layer over the South Atlantic during the OOMPH cruise in March 2007, *Atmos Chem Phys*, 15, 6971-6980, 2015.
- Fischer, H., Axinte, R., Bozem, H., Crowley, J. N., Ernest, C., Gilge, S., Hafermann, S., Harder, H., Hens, K., and Janssen, R. H.: Diurnal variability, photochemical production and loss processes of hydrogen peroxide in the boundary layer over Europe, *Atmos Chem Phys*, 19, 11953-11968, 2019.
- 475 Gao, J., Wang, H., Liu, W., Xu, H., Wei, Y., Tian, X., Feng, Y., Song, S., and Shi, G.: Hydrogen peroxide serves as pivotal fountainhead for aerosol aqueous sulfate formation from a global perspective, *Nat Commun*, 15, 4625, 10.1038/s41467-024-48793-1, 2024.
- 480 George, I. J., Matthews, P. S. J., Whalley, L. K., Brooks, B., Goddard, A., Baeza-Romero, M. T., and Heard, D. E.: Measurements of uptake coefficients for heterogeneous loss of HO₂ onto submicron inorganic salt aerosols, *Phys Chem Chem Phys*, 15, 12829-12845, 10.1039/C3CP51831K, 2013.
- 485 Guo, J., Wang, Z., Cui, Y., and Zhang, X.: Assessment of the H₂O₂ budget at an urban site concerning the HO₂ underprediction and the vertical transport from residual layers, *Atmos Environ*, 272, 118952, <https://doi.org/10.1016/j.atmosenv.2022.118952>, 2022.
- 490 Guo, J., Tilgner, A., Yeung, C., Wang, Z., Louie, P. K. K., Luk, C. W. Y., Xu, Z., Yuan, C., Gao, Y., Poon, S., Herrmann, H., Lee, S., Lam, K. S., and Wang, T.: Atmospheric Peroxides in a Polluted Subtropical Environment: Seasonal Variation, Sources and Sinks, and Importance of Heterogeneous Processes, *Environ Sci Technol*, 48, 1443-1450, 10.1021/es403229x, 2014.
- 495 He, S. Z., Chen, Z. M., Zhang, X., Zhao, Y., Huang, D. M., Zhao, J. N., Zhu, T., Hu, M., and Zeng, L. M.: Measurement of atmospheric hydrogen peroxide and organic peroxides in Beijing before and during the 2008 Olympic Games: Chemical and physical factors influencing their concentrations, *J Geophys Res-Atmos*, 115, ArtD17307, 10.1029/2009jd013544, 2010.
- 500 Hua, W., Chen, Z. M., Jie, C. Y., Kondo, Y., Hofzumahaus, A., Takegawa, N., Chang, C. C., Lu, K. D., Miyazaki, Y., Kita, K., Wang, H. L., Zhang, Y. H., and Hu, M.: Atmospheric hydrogen peroxide and organic hydroperoxides during PRIDE-PRD'06, China: their concentration, formation mechanism and contribution to secondary aerosols, *Atmos Chem Phys*, 8, 6755-6773, DOI 10.5194/acp-8-6755-2008, 2008.
- 505 Kanaya, Y., Cao, R., Akimoto, H., Fukuda, M., Komazaki, Y., Yokouchi, Y., Koike, M., Tanimoto, H., Takegawa, N., and Kondo, Y.: Urban photochemistry in central Tokyo: 1. Observed and modeled OH and HO₂ radical concentrations during the winter and summer of 2004, *Journal of Geophysical Research: Atmospheres*, 112, <https://doi.org/10.1029/2007JD008670>, 2007a.
- 510 Kanaya, Y., Tanimoto, H., Matsumoto, J., Furutani, H., Hashimoto, S., Komazaki, Y., Tanaka, S., Yokouchi, Y., Kato, S., Kajii, Y., and Akimoto, H.: Diurnal variations in H₂O₂, O₃, PAN, HNO₃ and aldehyde concentrations and NO/NO₂ ratios



- at Rishiri Island, Japan: Potential influence from iodine chemistry, *Sci Total Environ*, 376, 185-197, <https://doi.org/10.1016/j.scitotenv.2007.01.073>, 2007b.
- 515 Klippel, T., Fischer, H., Bozem, H., Lawrence, M. G., Butler, T., Jöckel, P., Tost, H., Martinez, M., Harder, H., and Regelin, E.: Distribution of hydrogen peroxide, methyl hydroperoxide and formaldehyde over central Europe during the HOOVER project, *Atmos Chem Phys*, 11, 4391-4410, 2011.
- 520 Lakey, P. S. J., George, I. J., Whalley, L. K., Baeza-Romero, M. T., and Heard, D. E.: Measurements of the HO₂ Uptake Coefficients onto Single Component Organic Aerosols, *Environ Sci Technol*, 49, 4878-4885, 10.1021/acs.est.5b00948, 2015.
- Lazrus, A. L., Kok, G. L., Lind, J. A., Gitlin, S. N., Heikes, B. G., and Shetter, R. E.: Automated Fluorometric Method for Hydrogen-Peroxide in Air, *Anal Chem*, 58, 594-597, Doi 10.1021/Ac00294a024, 1986.
- 525 Lee, G., Jang, Y., Lee, H., Han, J.-S., Kim, K.-R., and Lee, M.: Characteristic behavior of peroxyacetyl nitrate (PAN) in Seoul megacity, Korea, *Chemosphere*, 73, 619-628, <https://doi.org/10.1016/j.chemosphere.2008.05.060>, 2008a.
- Lee, M., Kie, J. A., Kim, Y. M., and Lee, G.: Characteristics of atmospheric hydrogen peroxide variations in Seoul megacity during 2002-2004, *Sci Total Environ*, 393, 299-308, 10.1016/j.scitotenv.2007.11.037, 2008b.
- 530 Li, J. R., Zhu, C., Chen, H., Fu, H. B., Xiao, H., Wang, X. F., Herrmann, H., and Chen, J. M.: A More Important Role for the Ozone-S(IV) Oxidation Pathway Due to Decreasing Acidity in Clouds, *J Geophys Res-Atmos*, 125, 2020.
- Li, K., Jacob, D. J., Liao, H., Shen, L., Zhang, Q., and Bates, K. H.: Anthropogenic drivers of 2013-2017 trends in summer surface ozone in China, *P Natl Acad Sci USA*, 116, 422-427, 10.1073/pnas.1812168116, 2019.
- 535 Liang, H., Chen, Z. M., Huang, D., Zhao, Y., and Li, Z. Y.: Impacts of aerosols on the chemistry of atmospheric trace gases: a case study of peroxides and HO₂ radicals, *Atmos Chem Phys*, 13, 11259-11276, 10.5194/acp-13-11259-2013, 2013.
- 540 Liu, P., Ye, C., Zhang, C., He, G., Xue, C., Liu, J., Liu, C., Zhang, Y., Song, Y., Li, X., Wang, X., Chen, J., He, H., Herrmann, H., and Mu, Y.: Photochemical Aging of Atmospheric Fine Particles as a Potential Source for Gas-Phase Hydrogen Peroxide, *Environ Sci Technol*, 55, 15063-15071, 10.1021/acs.est.1c04453, 2021.
- 545 Liu, Y., Geng, G., Cheng, J., Liu, Y., Xiao, Q., Liu, L., Shi, Q., Tong, D., He, K., and Zhang, Q.: Drivers of Increasing Ozone during the Two Phases of Clean Air Actions in China 2013–2020, *Environ Sci Technol*, 57, 8954-8964, 10.1021/acs.est.3c00054, 2023.
- Lu, X., Zhang, L., Wang, X., Gao, M., Li, K., Zhang, Y., Yue, X., and Zhang, Y.: Rapid Increases in Warm-Season Surface Ozone and Resulting Health Impact in China Since 2013, *Environmental Science & Technology Letters*, 7, 240-247, 2020.
- 550 Ma, X., Tan, Z., Lu, K., Yang, X., Chen, X., Wang, H., Chen, S., Fang, X., Li, S., Li, X., Liu, J., Liu, Y., Lou, S., Qiu, W., Wang, H., Zeng, L., and Zhang, Y.: OH and HO₂ radical chemistry at a suburban site during the EXPLORE-YRD campaign in 2018, *Atmos. Chem. Phys.*, 22, 7005-7028, 10.5194/acp-22-7005-2022, 2022.
- 555 Ma, Z., Xu, J., Quan, W., Zhang, Z., Lin, W., and Xu, X.: Significant increase of surface ozone at a rural site, north of eastern China, *Atmos. Chem. Phys.*, 16, 3969-3977, 10.5194/acp-16-3969-2016, 2016.
- 560 Nunnermacker, L. J., Weinstein-Lloyd, J. B., Hillery, B., Giebel, B., Kleinman, L. I., Springston, S. R., Daum, P. H., Gaffney, J., Marley, N., and Huey, G.: Aircraft and ground-based measurements of hydroperoxides during the 2006 MILAGRO field campaign, *Atmos Chem Phys*, 8, 7619-7636, 10.5194/acp-8-7619-2008, 2008.



- Peng, X., Wang, W., Xia, M., Chen, H., Ravishankara, A. R., Li, Q., Saiz-Lopez, A., Liu, P., Zhang, F., Zhang, C., Xue, L., Wang, X., George, C., Wang, J., Mu, Y., Chen, J., and Wang, T.: An unexpected large continental source of reactive bromine and chlorine with significant impact on wintertime air quality, *National Science Review*, 8, nwaa304, 10.1093/nsr/nwaa304, 2021.
- 565 Penkett, S. A., Jones, B. M. R., Brice, K. A., and Eggleton, A. E. J.: Importance of Atmospheric Ozone and Hydrogen-Peroxide in Oxidizing Sulfur-Dioxide in Cloud and Rainwater, *Atmos Environ*, 13, 123-137, Doi 10.1016/0004-6981(79)90251-8, 1979.
- 570 Pradhan, M., Kalberer, M., Griffiths, P. T., Braban, C. F., Pope, F. D., Cox, R. A., and Lambert, R. M.: Uptake of Gaseous Hydrogen Peroxide by Submicrometer Titanium Dioxide Aerosol as a Function of Relative Humidity, *Environ Sci Technol*, 44, 1360-1365, 10.1021/es902916f, 2010.
- Qin, M., Chen, Z., Shen, H., Li, H., Wu, H., and Wang, Y.: Impacts of heterogeneous reactions to atmospheric peroxides: Observations and budget analysis study, *Atmos Environ*, 183, 144-153, 10.1016/j.atmosenv.2018.04.005, 2018.
- 575 Qin, X., Chen, Z., Gong, Y., Dong, P., Cao, Z., Hu, J., and Xu, J.: Persistent Uptake of H₂O₂ onto Ambient PM_{2.5} via Dark-Fenton Chemistry, *Environ Sci Technol*, 56, 9978-9987, 10.1021/acs.est.2c03630, 2022.
- 580 Rao, Z., Fang, Y.-G., Pan, Y., Yu, W., Chen, B., Francisco, J. S., Zhu, C., and Chu, C.: Accelerated Photolysis of H₂O₂ at the Air–Water Interface of a Microdroplet, *Journal of the American Chemical Society*, 145, 24717-24723, 10.1021/jacs.3c08101, 2023.
- Reeves, C. E. and Penkett, S. A.: Measurements of peroxides and what they tell us, *Chem Rev*, 103, 5199-5218, 585 10.1021/cr0205053, 2003.
- Ren, Y., Ding, A. J., Wang, T., Shen, X. H., Guo, J., Zhang, J. M., Wang, Y., Xu, P. J., Wang, X. F., Gao, J., and Collett, J. L.: Measurement of gas-phase total peroxides at the summit of Mount Tai in China, *Atmos Environ*, 43, 1702-1711, 590 10.1016/j.atmosenv.2008.12.020, 2009.
- Romanias, M. N., El Zein, A., and Bedjanian, Y.: Heterogeneous Interaction of H₂O₂ with TiO₂ Surface under Dark and UV Light Irradiation Conditions, *The Journal of Physical Chemistry A*, 116, 8191-8200, 10.1021/jp305366v, 2012.
- Sillman, S.: The use of NO_y, H₂O₂, and HNO₃ as indicators for ozone-NO_x-hydrocarbon sensitivity in urban locations, 595 *Journal of Geophysical Research: Atmospheres*, 100, 14175-14188, 1995.
- Sillman, S., He, D., Pippin, M. R., Daum, P. H., Imre, D. G., Kleinman, L. I., Lee, J. H., and Weinstein-Lloyd, J.: Model correlations for ozone, reactive nitrogen, and peroxides for Nashville in comparison with measurements: Implications for O₃-NO_x-hydrocarbon chemistry, *Journal of Geophysical Research: Atmospheres*, 103, 22629-22644, 1998.
- 600 Sofen, E. D., Alexander, B., and Kunasek, S. A.: The impact of anthropogenic emissions on atmospheric sulfate production pathways, oxidants, and ice core $\Delta\text{O}^{17}(\text{SO}_4^{2-})$, *Atmos. Chem. Phys.*, 11, 3565-3578, 10.5194/acp-11-3565-2011, 2011.
- Song, H., Lu, K., Dong, H., Tan, Z., Chen, S., Zeng, L., and Zhang, Y.: Reduced Aerosol Uptake of Hydroperoxyl Radical May Increase the Sensitivity of Ozone Production to Volatile Organic Compounds, *Environmental Science & Technology Letters*, 9, 22-29, 10.1021/acs.estlett.1c00893, 2022.
- 605 Sun, M., Cui, J. n., Zhao, X., and Zhang, J.: Impacts of precursors on peroxyacetyl nitrate (PAN) and relative formation of PAN to ozone in a southwestern megacity of China, *Atmos Environ*, 231, 117542, 610 <https://doi.org/10.1016/j.atmosenv.2020.117542>, 2020.



- Takami, A., Shiratori, N., Yonekura, H., and Hatakeyama, S.: Measurement of hydroperoxides and ozone in Oku-Nikko area, *Atmos Environ*, 37, 3861-3872, 10.1016/S1352-2310(03)00454-0, 2003.
- 615 Taketani, F., Kanaya, Y., Pochanart, P., Liu, Y., Li, J., Okuzawa, K., Kawamura, K., Wang, Z., and Akimoto, H.: Measurement of overall uptake coefficients for HO₂ radicals by aerosol particles sampled from ambient air at Mts. Tai and Mang (China), *Atmos. Chem. Phys.*, 12, 11907-11916, 10.5194/acp-12-11907-2012, 2012.
- 620 Tan, Z., Hofzumahaus, A., Lu, K., Brown, S. S., Holland, F., Huey, L. G., Kiendler-Scharr, A., Li, X., Liu, X., Ma, N., Min, K.-E., Rohrer, F., Shao, M., Wahner, A., Wang, Y., Wiedensohler, A., Wu, Y., Wu, Z., Zeng, L., Zhang, Y., and Fuchs, H.: No Evidence for a Significant Impact of Heterogeneous Chemistry on Radical Concentrations in the North China Plain in Summer 2014, *Environ Sci Technol*, 54, 5973-5979, 10.1021/acs.est.0c00525, 2020.
- 625 Tan, Z., Fuchs, H., Lu, K., Hofzumahaus, A., Bohn, B., Broch, S., Dong, H., Gomm, S., Häsel, R., He, L., Holland, F., Li, X., Liu, Y., Lu, S., Rohrer, F., Shao, M., Wang, B., Wang, M., Wu, Y., Zeng, L., Zhang, Y., Wahner, A., and Zhang, Y.: Radical chemistry at a rural site (Wangdu) in the North China Plain: observation and model calculations of OH, HO₂ and RO₂ radicals, *Atmos. Chem. Phys.*, 17, 663-690, 10.5194/acp-17-663-2017, 2017.
- 630 Tang, M. J., Huang, X., Lu, K. D., Ge, M. F., Li, Y. J., Cheng, P., Zhu, T., Ding, A. J., Zhang, Y. H., Gligorovski, S., Song, W., Ding, X., Bi, X. H., and Wang, X. M.: Heterogeneous reactions of mineral dust aerosol: implications for tropospheric oxidation capacity, *Atmos Chem Phys*, 17, 11727-11777, 10.5194/acp-17-11727-2017, 2017.
- 635 Thornton, J. A., Jaeglé, L., and McNeill, V. F.: Assessing known pathways for HO₂ loss in aqueous atmospheric aerosols: Regional and global impacts on tropospheric oxidants, *Journal of Geophysical Research: Atmospheres*, 113, <https://doi.org/10.1029/2007JD009236>, 2008.
- 640 Trainer, M., Parrish, D. D., Buhr, M. P., Norton, R. B., Fehsenfeld, F. C., Anlauf, K. G., Bottenheim, J. W., Tang, Y. Z., Wiebe, H. A., Roberts, J. M., Tanner, R. L., Newman, L., Bowersox, V. C., Meagher, J. F., Olszyna, K. J., Rodgers, M. O., Wang, T., Berresheim, H., Demerjian, K. L., and Roychowdhury, U. K.: Correlation of ozone with NO_y in photochemically aged air, *Journal of Geophysical Research: Atmospheres*, 98, 2917-2925, <https://doi.org/10.1029/92JD01910>, 1993.
- 645 Walker, S. J., Evans, M. J., Jackson, A. V., Steinbacher, M., Zellweger, C., and McQuaid, J. B.: Processes controlling the concentration of hydroperoxides at Jungfraujoch Observatory, Switzerland, *Atmos Chem Phys*, 6, 5525-5536, DOI 10.5194/acp-6-5525-2006, 2006.
- 650 Wang, T., Ding, A., Gao, J., and Wu, W. S.: Strong ozone production in urban plumes from Beijing, China, *Geophys Res Lett*, 33, 2006.
- 655 Wang, W., Li, X., Shao, M., Hu, M., Zeng, L., Wu, Y., and Tan, T.: The impact of aerosols on photolysis frequencies and ozone production in Beijing during the 4-year period 2012–2015, *Atmos. Chem. Phys.*, 19, 9413-9429, 10.5194/acp-19-9413-2019, 2019.
- Wang, W., Parrish, D. D., Li, X., Shao, M., Liu, Y., Mo, Z., Lu, S., Hu, M., Fang, X., Wu, Y., Zeng, L., and Zhang, Y.: Exploring the drivers of the increased ozone production in Beijing in summertime during 2005–2016, *Atmos. Chem. Phys.*, 20, 15617-15633, 10.5194/acp-20-15617-2020, 2020.
- Wang, Y., Chen, Z. M., Wu, Q. Q., Liang, H., Huang, L. B., Li, H., Lu, K. D., Wu, Y. S., Dong, H. B., Zeng, L. M., and Zhang, Y. H.: Observation of atmospheric peroxides during Wangdu Campaign 2014 at a rural site in the North China Plain, *Atmos Chem Phys*, 16, 10985-11000, 10.5194/acp-16-10985-2016, 2016.



- 660 Watanabe, K., Yachi, C., Nishibe, M., Michigami, S., Saito, Y., Eda, N., Yamazaki, N., and Hirai, T.: Measurements of atmospheric hydroperoxides over a rural site in central Japan during summers using a helicopter, *Atmos Environ*, 146, 174-182, 2016.
- 665 Watkins, B. A., Parrish, D. D., Buhr, S., Norton, R. B., Trainer, M., Yee, J. E., and Fehsenfeld, F. C.: Factors influencing the concentration of gas phase hydrogen peroxide during the summer at Kinterbish, Alabama, *Journal of Geophysical Research: Atmospheres*, 100, 22841-22851, <https://doi.org/10.1029/95JD01533>, 1995.
- 670 Whalley, L. K., Furneaux, K. L., Goddard, A., Lee, J. D., Mahajan, A., Oetjen, H., Read, K. A., Kaaden, N., Carpenter, L. J., Lewis, A. C., Plane, J. M. C., Saltzman, E. S., Wiedensohler, A., and Heard, D. E.: The chemistry of OH and HO₂ radicals in the boundary layer over the tropical Atlantic Ocean, *Atmos. Chem. Phys.*, 10, 1555-1576, 10.5194/acp-10-1555-2010, 2010.
- 675 Xu, W., Zhang, G., Wang, Y., Tong, S., Zhang, W., Ma, Z., Lin, W., Kuang, Y., Yin, L., and Xu, X.: Aerosol Promotes Peroxyacetyl Nitrate Formation During Winter in the North China Plain, *Environ Sci Technol*, 55, 3568-3581, 10.1021/acs.est.0c08157, 2021.
- 680 Xue, C., Ye, C., Kleffmann, J., Zhang, W., He, X., Liu, P., Zhang, C., Zhao, X., Liu, C., Ma, Z., Liu, J., Wang, J., Lu, K., Catoire, V., Mellouki, A., and Mu, Y.: Atmospheric measurements at Mt. Tai – Part II: HONO budget and radical (RO_x+NO₃) chemistry in the lower boundary layer, *Atmos. Chem. Phys.*, 22, 1035-1057, 10.5194/acp-22-1035-2022, 2022.
- Xue, C. Y., Zhang, C. L., Ye, C., Liu, P. F., Catoire, V., Krysztofiak, G., Chen, H., Ren, Y. G., Zhao, X. X., Wang, J. H., Zhang, F., Zhang, C. X., Zhang, J. W., An, J. L., Wang, T., Chen, J. M., Kleffmann, J., Mellouki, A., and Mu, Y. J.: HONO Budget and Its Role in Nitrate Formation in the Rural North China Plain, *Environ Sci Technol*, 54, 11048-11057, 2020.
- 685 Ye, C., Liu, P., Ma, Z., Xue, C., Zhang, C., Zhang, Y., Liu, J., Liu, C., Sun, X., and Mu, Y.: High H₂O₂ Concentrations Observed during Haze Periods during the Winter in Beijing: Importance of H₂O₂ Oxidation in Sulfate Formation, *Environmental Science & Technology Letters*, 10.1021/acs.estlett.8b00579, 2018.
- 690 Ye, C., Xue, C., Liu, P., Zhang, C., Ma, Z., Zhang, Y., Liu, C., Liu, J., Lu, K., and Mu, Y.: Strong impacts of biomass burning, nitrogen fertilization, and fine particles on gas-phase hydrogen peroxide (H₂O₂), *Sci Total Environ*, 843, 156997, <https://doi.org/10.1016/j.scitotenv.2022.156997>, 2022.
- 695 Ye, C., Xue, C., Zhang, C., Ma, Z., Liu, P., Zhang, Y., Liu, C., Zhao, X., Zhang, W., He, X., Song, Y., Liu, J., Wang, W., Sui, B., Cui, R., Yang, X., Mei, R., Chen, J., and Mu, Y.: Atmospheric Hydrogen Peroxide (H₂O₂) at the Foot and Summit of Mt. Tai: Variations, Sources and Sinks, and Implications for Ozone Formation Chemistry, *Journal of Geophysical Research: Atmospheres*, 126, e2020JD033975, <https://doi.org/10.1029/2020JD033975>, 2021a.
- 700 Ye, C., Chen, H., Hoffmann, E. H., Mettke, P., Tilgner, A., He, L., Mutzel, A., Brüggemann, M., Poulain, L., Schaefer, T., Heinold, B., Ma, Z., Liu, P., Xue, C., Zhao, X., Zhang, C., Zhang, F., Sun, H., Li, Q., Wang, L., Yang, X., Wang, J., Liu, C., Xing, C., Mu, Y., Chen, J., and Herrmann, H.: Particle-Phase Photoreactions of HULIS and TMIs Establish a Strong Source of H₂O₂ and Particulate Sulfate in the Winter North China Plain, *Environ Sci Technol*, 55, 7818-7830, 10.1021/acs.est.1c00561, 2021b.
- 705 Zhang, G., Mu, Y. J., Liu, J. F., Zhang, C. L., Zhang, Y. Y., Zhang, Y. J., and Zhang, H. X.: Seasonal and diurnal variations of atmospheric peroxyacetyl nitrate, peroxypropionyl nitrate, and carbon tetrachloride in Beijing, *J Environ Sci-China*, 26, 65-74, 10.1016/S1001-0742(13)60382-4, 2014.



710 Zhang, Q., Liu, J., He, Y., Yang, J., Gao, J., Liu, H., Tang, W., Chen, Y., Fan, W., Chen, X., Chai, F., and Hatakeyama, S.:
Measurement of hydrogen peroxide and organic hydroperoxide concentrations during autumn in Beijing, China, J Environ
Sci-China, 64, 72-81, <https://doi.org/10.1016/j.jes.2016.12.015>, 2018.

715 Zhang, X., He, S. Z., Chen, Z. M., Zhao, Y., and Hua, W.: Methyl hydroperoxide (CH₃OOH) in urban, suburban and rural
atmosphere: ambient concentration, budget, and contribution to the atmospheric oxidizing capacity, Atmos. Chem. Phys., 12,
8951-8962, 10.5194/acp-12-8951-2012, 2012.